

A Dynamic Programming Framework for Optimal Planning of Redundant Robots Along Prescribed Paths With Kineto-Dynamic Constraints

Enrico Ferrentino¹, Heitor J. Savino², Antonio Franchi³, Pasquale Chiacchio¹

Abstract—Off-line optimal planning of trajectories for redundant robots along prescribed task space paths is usually broken down into two consecutive processes: first, the task space path is inverted to obtain a joint-space path, then, the latter is parametrized with a time law. If the two processes are separated, they cannot optimize the same objective function, ultimately providing sub-optimal results. In this paper, a unified approach is presented where dynamic programming is the underlying optimization technique. Its flexibility allows accommodating arbitrary constraints and objective functions, thus providing a generic framework for optimal planning of real systems. To demonstrate its applicability to a real world scenario, the framework is instantiated for time-optimality. Compared to numerical solvers, the proposed methodology provides visibility of the underlying resolution process, allowing for further analyses beyond the computation of the optimal trajectory. The effectiveness of the framework is demonstrated on a real 7-degrees-of-freedom serial chain. The issues associated with the execution of optimal trajectories on a real controller are also discussed and addressed. The experiments show that the proposed framework is able to effectively exploit kinematic redundancy to optimize the performance index defined at planning level and generate feasible trajectories that can be executed on real hardware with satisfactory results.

I. INTRODUCTION

Kinematically redundant manipulators possess more degrees of freedom than those strictly required to execute a given task. Such a characteristic gives the system a higher degree of dexterity and mobility that can be exploited to optimize performance indices of interest. Such an optimization seeks the optimal inverse kinematics solution from an infinite set and is commonly referred to as *redundancy resolution*.

Many robotic tasks require to follow a specific path, such as in welding, cutting, gluing and in some assembly and disassembly tasks. The definition of the speed with which the path is tracked is also a decision variable that, in most applications, is necessary to optimize. Such an optimization seeks the optimal time law and is commonly referred to as *optimal trajectory planning* or *optimal time parametrization*.

Whether they are executed on-line or off-line, redundancy resolution and trajectory planning have been mostly treated

as two independent, consecutive optimization processes [1], [2], [3]. A workspace path is given, that is mapped, through inverse kinematics, in the joint space (possibly optimizing a geometric quality index), then, the joint-space path is time-parametrized to yield a trajectory (respecting constraints and possibly optimizing a different quality index), that can be executed through motion control at joint level. The optimization performed at the former stage can be functional to the optimization performed at the latter. Overall, the two processes “cooperate” to achieve a common objective. Unfortunately, the resolution of two independent optimal problems does not guarantee the achievement of the overall optimal solution. Hence, the objective of this paper is to provide a unified formulation for both optimization problems, so that kinematic redundancy is effectively exploited for the minimization/maximization of the objective function defined at trajectory planning level.

The foundations of optimal trajectory planning were laid for time minimization and non-redundant robots [4], [5], [6], and later extended to kinematically redundant systems, such as in [7], [8]. Here, the time-optimal problem is solved numerically by making use of the *Extended Pontryagin’s Maximum Principle (EPMP)* and considering an approximation of the torque constraints, but the formulation is inflexible with respect to the introduction of additional constraints and objective functions. In [9], a try-and-error approach is proposed. Because of the bang-bang hypothesis, objective functions other than tracking time cannot be considered. In addition, for the sake of efficiency, the number of switching points is possibly reduced with respect to the real time-optimal trajectory. Lastly, the algorithm cannot enforce zero joint velocity at the end of the motion, which is undesirable in most applications. A different approach consists in addressing the optimization problem directly with multiple shooting [10], after an initial guess on the optimization variables is made. Since the problem is non-convex, globally-optimal solutions cannot be guaranteed and, in general, the quality of the resulting solution strictly depends on the initial guess. On the other hand, the formulation is flexible enough to include constraints on the joint positions and their derivatives, as well as other application-specific constraints.

This paper adopts dynamic programming (DP) as the main underlying methodology and central idea to cope with the complexity of reality. Also, because of its employment, in previous works, for both the optimization problems described above, it naturally arises as the unifying approach (see, for instance, [11], [12], [13], [14], [15] for redundancy resolution, and [16], [17], [18], [19] for trajectory planning). Dynamic

¹E. Ferrentino and P. Chiacchio are with the Department of Computer and Electrical Engineering and Applied Mathematics (DIEM), University of Salerno, Fisciano, SA, 84084, Italy, {eferrentino, pchiacchio}@unisa.it

²H. J. Savino is with Ambev ZBS SAZ, Jacaré, SP, 12334-480, Brazil, heitor.savino@ambev.com.br

³A. Franchi is with LAAS-CNRS, Université de Toulouse, CNRS, Toulouse, 31400, France, and also with the Robotics and Mechatronics Laboratory, Faculty of Electrical Engineering, Mathematics & Computer Science, University of Twente, Enschede 7522NH, The Netherlands, a.franchi@utwente.nl

programming is extremely flexible in the accommodation of arbitrary constraints and objective functions and, compatibly with the available planning time, can guarantee global optimality [20]. When applied to real systems, it well describes the constraints at hand and no conservative hypotheses are necessary. With respect to other numerical techniques, it allows for deeper insights of the optimal solution, such as the visualization of the null-space associated with redundancy and of the phase-plane trajectory, that are key aspects to assess feasibility and optimality.

The problem is formalized in a discrete state space, where the redundancy dimension is parametrized with a minimal representation and combined with the pseudo-velocity (time derivative of the arc length) dimension. The DP setting is thus transformed into a graph search problem where the admissible inputs are only those driving the system towards states in the graph. We include kineto-dynamic constraints and formalize them in a way that graph nodes become unreachable when they are violated. The problem is then solved through approximate DP. These matters are addressed in Section II. The algorithmic implementation of our methodology is presented in Section III, while its effectiveness is discussed in Section IV through experiments on a real 7 degrees of freedom (DOF) robotic manipulator. Here, a comparison is made with an algorithm from [1], that performs redundancy resolution and time parametrization in two separate stages. Section V concludes our work and sketches some ideas for further developments.

II. PROBLEM FORMULATION

A. State space definition

Let us consider a geometrical path for the end-effector $\mathbf{x}(\lambda) : [0, L] \rightarrow \mathbb{R}^m$, such that a given manipulator with n degrees of freedom is redundant, i.e. $n > m$. It follows that $r = n - m$, the *redundancy degree*, is strictly greater than zero. λ is the arc length, L is the path length. The joint positions along the path $\mathbf{q}(\lambda) \in \mathbb{R}^n$ are unknown, as well as the time law $\lambda(t) : \mathbb{R} \rightarrow [0, L]$ associated with them. The time derivative of the arc length $\dot{\lambda} = \frac{d\lambda}{dt}$ encodes the time information, and, when expressed as $\dot{\lambda}(\lambda)$, for variable λ , it is often referred to as *phase plane trajectory* (PPT) [4], [5].

Let us discretize λ in space with a given step Δ_λ , i.e.,

$$\lambda(i) = i\Delta_\lambda, \quad \text{with } i = 0, 1, 2, \dots, N_i \quad \text{and } \Delta_\lambda = \frac{L}{N_i} \quad (1)$$

such that $\mathbf{x}(\lambda(i)) = \mathbf{x}(i)$ can be viewed as the $(i + 1)$ -th waypoint. i is termed *stage index*.

The robot dynamic model is given by

$$\boldsymbol{\tau}(i) = \mathbf{H}(\mathbf{q}(i))\ddot{\mathbf{q}}(i) + \mathbf{f}(\mathbf{q}(i), \dot{\mathbf{q}}(i)), \quad (2)$$

where, $\mathbf{f}(\mathbf{q}, \dot{\mathbf{q}})$ is the $n \times 1$ vector including centrifugal and Coriolis contributions, Coulomb and viscous friction terms, and gravitational torques.

Let $S_{(\cdot)}(i)$ be the discrete-time (vectorial) function (or *sequence* of samples) of the continuous-time (vectorial) function $(\cdot)(\lambda)$ up until the i -th sample. The joint velocities and accelerations at a given stage i , $\dot{\mathbf{q}}(i)$ and $\ddot{\mathbf{q}}(i)$ respectively, in a discrete-time formulation, can be approximated, through

fixed-step integration schemes, as functions of the sequences $S_{\mathbf{q}}(i)$, $S_{\dot{\mathbf{q}}}(i)$ and $S_t(i)$, i.e.,

$$\dot{\mathbf{q}}(i) \sim f_{\dot{\mathbf{q}}}(S_{\mathbf{q}}(i), S_t(i)), \quad (3)$$

$$\ddot{\mathbf{q}}(i) \sim f_{\ddot{\mathbf{q}}}(S_{\dot{\mathbf{q}}}(i), S_t(i)). \quad (4)$$

The exact form of the functions above depends on the specific integration scheme. We note here, and further clarify in Section III, that derivatives are assumed to be computed with past samples, in a backward integration scheme, because future samples, in a forward optimization scheme, are unknown, as they depend on optimal choices that yet have to be made.

In the same way, each timestamp in $S_t(i)$ can be derived from the phase plane trajectory, through some discrete approximation, e.g. the trapezoidal approximation used in [17], that generically is

$$t(i) \sim f_t(S_\lambda(i), S_{\dot{\lambda}}(i)). \quad (5)$$

Let us remark, once again, that $S_{\dot{\lambda}}(i)$ is unknown and, as a consequence, $t(i)$ is unknown too.

Let us define the *forward kinematics function* $\mathbf{k}(\mathbf{q}) : \mathbb{R}^n \rightarrow \mathbb{R}^m$. The path constraint at the given waypoints is

$$\mathbf{x}(i) = \mathbf{k}(\mathbf{q}(i)). \quad (6)$$

Through *joint space decomposition* (JSD), the redundancy parameters are selected from the joint positions. Under this hypothesis, each of the joint positions in $S_{\mathbf{q}}(i)$ in (3) can be computed from non-redundant inverse kinematics (IK) as

$$\mathbf{q}(i) = \mathbf{k}^{-1}(\mathbf{x}(i), \mathbf{v}(i), g(i)), \quad (7)$$

where $\mathbf{v} \in \mathbb{R}^r$ is the vector of redundancy parameters. Since more than one configuration may satisfy the non-redundant IK, g selects the specific IK solution to be considered at stage i . This way defined, $\mathbf{q}(i)$ is unique. Since \mathbf{x} is a function of λ , we may rewrite the equation above as

$$\mathbf{q}(i) = \mathbf{k}^{-1}(\lambda(i), \mathbf{v}(i), g(i)). \quad (8)$$

Now, we may fold (5) and (8), for each i , into (3) and (4), yielding

$$\dot{\mathbf{q}}(i) \sim f_{\dot{\mathbf{q}}}(S_\lambda(i), S_{\dot{\lambda}}(i), S_{\mathbf{v}}(i), S_g(i)), \quad (9)$$

$$\ddot{\mathbf{q}}(i) \sim f_{\ddot{\mathbf{q}}}(S_\lambda(i), S_{\dot{\lambda}}(i), S_{\mathbf{v}}(i), S_g(i)). \quad (10)$$

By substituting both equations above into (2), we find that, in general, the torques are functions of the four identified sequences, i.e.

$$\boldsymbol{\tau}(i) \sim f_{\boldsymbol{\tau}}(S_\lambda(i), S_{\dot{\lambda}}(i), S_{\mathbf{v}}(i), S_g(i)). \quad (11)$$

This means that, given the current state at stage i , selecting the input $\boldsymbol{\tau}(i)$ that drives the discrete-time system to another state is equivalent to selecting the parameters λ , \mathbf{v} and g at the next stage. This is coherent with the logic of discretizing the state space instead of the input space that is common to all the previous works using DP for redundancy resolution and time-optimal planning. Notoriously, this is also a way to control the curse of dimensionality, that is a well-known issue in DP. λ , \mathbf{v} and g also constitute a minimum parametrization of the state for each stage, as opposed to [7] and [21] that,

rather, use redundant representations.

Thus, let us proceed by discretizing the variables $\dot{\lambda}$ and \mathbf{v} . The former is

$$\dot{\lambda}_l = l\Delta_{\dot{\lambda}}, \quad \text{with } l = 0, 1, 2, \dots, N_l \quad \text{and } \Delta_{\dot{\lambda}} = \frac{\dot{\lambda}_M}{N_l}, \quad (12)$$

where $\dot{\lambda}_M$ is the maximum pseudo-velocity value that the phase plane trajectory can reach. The latter is

$$\mathbf{v} = \mathbf{j} \circ \mathbf{\Delta}_v + \mathbf{v}_{min}, \quad (13)$$

where ‘ \circ ’ denotes the Hadamard product, $\mathbf{\Delta}_v = [\Delta_{v,1}, \dots, \Delta_{v,r}]$ is the vector of the sampling intervals, $\mathbf{j} \in \mathbb{N}^r$ the vector of the redundancy parameter indices, and \mathbf{v}_{min} is the vector of lower bounds of the redundancy parameters domains. The elements of \mathbf{j} take the maximum values $N_{j,1}, \dots, N_{j,r}$ so that $[N_{j,1}, \dots, N_{j,r}] \circ \mathbf{\Delta}_v + \mathbf{v}_{min}$ equals the upper bound of the redundant joint domains.

The discretized domains of λ , $\dot{\lambda}$, \mathbf{v} and g (the latter is naturally discrete) make up a grid of $r + 3$ dimensions. We essentially adopt the same approach as other DP formulations for redundancy resolution and time-optimal planning, but we increase the number of dimensions to take into account: (1) the resolution of both problems together; (2) the presence of multiple inverse kinematics solutions. Each node in the grid will then contain a state given by

$$\mathbf{s}_{ljg}(i) = [\dot{\lambda}_l(i), \mathbf{q}_{jg}(i)], \quad (14)$$

where \mathbf{q}_{jg} is the vector of joint positions obtained from (8) using the redundancy parameters \mathbf{v}_j and selecting the IK solution (or *extended aspect* [15]) g .

B. Constraints

DP algorithms are extremely flexible with respect to the inclusion of arbitrary constraints. Common constraints are limits on joint positions and their derivatives, actuation constraints, obstacles in the workspace, velocity and acceleration limits in the Cartesian space, initial/final joint configurations, cyclicity (for closed workspace paths), power limits, maximum/minimum forces exchanged with the environment in an interaction scenario. Many other constraints can be designed depending on the specific application at hand. In the experiments that will follow in Section IV, we consider minimum/maximum joint positions, maximum joint velocities, accelerations, jerks, torques and torque rates.

Let us define the stage-dependent set \mathcal{A}_i , containing all the nodes returning joint positions that respect the joint domains, the path constraint and, possibly, imposed initial/final configurations. Such constraints are formalized as

$$\mathbf{s}_{ljg}(i) \in \mathcal{A}_i. \quad (15)$$

Joint velocity, acceleration and jerk limits can be directly encoded in equivalent stage-dependent, as well as state-dependent sets \mathcal{B}_i^1 , \mathcal{B}_i^2 and \mathcal{B}_i^3 , so that:

$$\dot{\mathbf{q}}(i) \in \mathcal{B}_i^1(\mathbf{s}(i)), \quad (16)$$

$$\ddot{\mathbf{q}}(i) \in \mathcal{B}_i^2(\mathbf{s}(i)), \quad (17)$$

$$\dddot{\mathbf{q}}(i) \in \mathcal{B}_i^3(\mathbf{s}(i)). \quad (18)$$

Equivalently, joint torque and torque rate limits can be encoded in similar sets \mathcal{C}_i^1 and \mathcal{C}_i^2 :

$$\boldsymbol{\tau}(i) \in \mathcal{C}_i^1(\mathbf{s}(i)), \quad (19)$$

$$\dot{\boldsymbol{\tau}}(i) \in \mathcal{C}_i^2(\mathbf{s}(i)). \quad (20)$$

More commonly, all the quantities above are given within fixed domains that do not change along the trajectory, are not configuration dependent, and not velocity-dependent, but the generality of the framework allows for the accommodation of more complex constraints. For example, interacting torque constraints, that cannot be parametrized [16], can be easily handled with DP.

All the sets above can be combined together to define the set \mathcal{D}_i of reachable states for a generic stage i , that is

$$\mathcal{D}_i = \mathcal{A}_i \cap \left\{ \mathbf{s}(i) : \dot{\mathbf{q}}(i) \in \mathcal{B}_i^1, \ddot{\mathbf{q}}(i) \in \mathcal{B}_i^2, \ddot{\mathbf{q}}(i) \in \mathcal{B}_i^3, \right. \\ \left. \boldsymbol{\tau}(i) \in \mathcal{C}_i^1, \dot{\boldsymbol{\tau}}(i) \in \mathcal{C}_i^2 \right. \\ \left. \text{with } \mathbf{s}(i-1) \in \mathcal{A}_{i-1}, \dots, \mathbf{s}(0) \in \mathcal{A}_0 \right\}. \quad (21)$$

C. Dynamic programming problem

Since all the states are available in the grid, the DP problem is transformed into a graph search problem [12], [14], [11]. This allows to adopt either a forward or a backward optimization scheme [15]. The objective function to optimize can be generally defined as

$$I(N_i) = \psi(\mathbf{s}_0) + \sum_{k=1}^{N_i} \phi(\mathbf{s}(k-1), \mathbf{s}(k)), \quad (22)$$

where $\psi(\mathbf{s}_0)$ is a cost associated to the initial state and ϕ is the cost computed locally between two adjacent states.

If, for instance, the objective function to minimize is the time, there is no cost associated to the initial state, i.e. $\psi(\mathbf{s}_0) = 0$ and $I = t$. Assuming a backward Euler approximation, (22) becomes

$$t(N_i) = \sum_{k=1}^{N_i} \frac{\lambda(k) - \lambda(k-1)}{\dot{\lambda}(k)}. \quad (23)$$

A different approximation can be adopted at the beginning and at the end of the trajectory to cope with the case $\dot{\lambda} = 0$ [17].

To complete our formulation, we rewrite (23) in a recursive form and use the set \mathcal{D}_i in (21), by minimizing over the admissible states:

$$t_{opt}(0) = 0,$$

$$t_{opt}(i) = \min_{\mathbf{s}(i) \in \mathcal{D}_i} \left[t_{opt}(i-1) + \frac{\lambda(i) - \lambda(i-1)}{\dot{\lambda}(i)} \right], \quad (24)$$

where $t_{opt}(i)$ at a generic stage i is the *optimal return function* (or *value function*) and $t_{opt}(N_i)$ represents the optimal cost.

III. ALGORITHMIC IMPLEMENTATION

Based on the problem formulation above, we can define the time-optimal trajectory planning algorithm for redundant

robots (TOTP-R) with DP as in Algorithm 1.

Algorithm 1 DP TOTP-R algorithm.

- 1: Initialize state space grid through inverse kinematics and discretization of λ , according to (8) and (14)
 - 2: Initialize $\mathcal{A}_i, \forall i = 0..(N_i - 1)$
 - 3: Initialize $\mathcal{B}_i^1, \mathcal{B}_i^2, \mathcal{B}_i^3, \mathcal{C}_i^1, \mathcal{C}_i^2 \forall i = 0..(N_i - 1)$ with state-independent information
 - 4: Initialize $\mathcal{D}_i = \emptyset, \forall i = 0..N_i$
 - 5: Initialize cost map $t_{i,l,j,g} = +\infty \forall i, l, j, g$
 - 6: $t_{0,l,j,g} \leftarrow 0 \forall l, j, g$
 - 7: $\mathcal{D}_0 \leftarrow \mathcal{A}_0$
 - 8: **for** $i \leftarrow 0$ to $N_i - 1$ **do**
 - 9: **for each** $s_{ijg} \in \mathcal{D}_i$ **do**
 - 10: **for each** $s_{mkh} \in \mathcal{A}_{i+1}$ **do**
 - 11: Compute $\dot{\mathbf{q}}, \ddot{\mathbf{q}}, \dot{\mathbf{q}}, \boldsymbol{\tau}, \dot{\boldsymbol{\tau}}$
 - 12: **if** Constraints in (16) - (20) are satisfied **then**
 - 13: $\mathcal{D}_{i+1} \leftarrow \mathcal{D}_{i+1} \cup \{s_{mkh}\}$
 - 14: Compute instantaneous cost function ϕ
 - 15: **if** $t_{i,l,j,g} + \phi < t_{i+1,m,k,h}$ **then**
 - 16: $t_{i+1,m,k,h} \leftarrow t_{i,l,j,g} + \phi$
 - 17: Let s_{ijg} at stage i be the predecessor of s_{mkh}
 - at stage $i + 1$
 - 18: $t_{opt}(N_i) \leftarrow \min_{j,g} [t_{N_i,0,j,g}]$
 - 19: Build functions $\lambda(i)$ and $\mathbf{q}(i)$ of optimal pseudo-velocities and joint positions by screening the predecessors map backward
-

The algorithm assumes that a workspace path is given as a discrete set of points and that they are associated to discrete values of the curvilinear coordinate, from $\lambda = 0$ to $\lambda = L$. If this is not the case, but some analytic curve is given, it can be sampled at the desired rate. At step 1, the redundancy parameters vector is discretized according to (13), which allows to compute IK solutions as in (8). The pseudo-velocity is also discretized according to (12), so that the grid nodes can be defined as in (14).

Usually, with reference to (8), analytic IK solvers are such that all the IK solutions for all extended aspects are obtained at once with one call to the solver, but, if this is not the case, or an analytic solver is not available, a condition should be specified by which one and only one IK solution is available for a given combination of redundancy parameters and workspace pose [15]. The grid index g selects such conditions/IK solutions.

At step 2, the nodes in the grid are enabled/disabled according to geometrical constraints including, for example, configurations that bring the robot to collide with the surrounding environment. Also, when a-priori information on the environment the robot is working in is available, entire grids can be excluded to make the DP algorithm find a trajectory in specific extended aspects, e.g. to keep a specific configuration of the elbow joint. The sets \mathcal{A}_i can also be used to impose that the robot must start and finish its motion at rest, or even stop along the path if this is required by the specific task.

In most practical cases, constraints on joint velocities, accelerations, jerks, torques, and torque rates are given in terms of state-independent connected sets, e.g. $\dot{\mathbf{q}} \in [\dot{\mathbf{q}}_{min}, \dot{\mathbf{q}}_{max}]$. In this case, the sets in (16)-(20) are completely defined beforehand, as done at step 3. Conversely, if they were state-dependent, they could be re-computed at the time

the constraints are checked, when the current velocity and acceleration of the system are known.

At a given stage i , for each pair of consecutive nodes (steps 9 and 10) the discrete-time functions (or sequences) of parameters $S_\lambda(i), S_{\dot{\lambda}}(i), S_v(i), S_g(i)$ are available through back-pointers to compute joint velocities, accelerations and torques as in (9)-(11) respectively, as well as joint jerks and torque rates with equivalent discrete approximations. If constraints are satisfied, we say that the node $s_{mkh}(i + 1)$ can be reached by the node $s_{ijg}(i)$. The former is then added to the set of nodes \mathcal{D}_{i+1} that can be visited at the next stage (step 13). Among all the nodes at stage i that can reach $s_{mkh}(i + 1)$, at step 17, we save the pointer to the one that provides the lowest cumulative cost (or optimal return function), according to (24).

After the process above has been repeated for all the workspace points, the one with minimum cumulative traversing time is picked (step 18) and, from it, the information about the time law, i.e. $\lambda(i)$, and exploitation of the null-space, i.e. $\mathbf{q}(i)$, are retrieved by following the map of predecessors backwards (step 19). The timestamps can be computed through (5) and applied to the joint-space path to obtain the optimal joint-space trajectory. Likewise, optimal joint velocities, accelerations, and torques can be computed from (9)-(11).

A few considerations are worthwhile. The enforcement of higher-order derivative constraints, like (18) and (20), would in principle require the introduction of an additional axis corresponding to the pseudo-acceleration $\ddot{\lambda}$ [16], [22], however this might make the problem intractable from the practical standpoint. In [18], continuous and differentiable profiles are generated in the phase plane through interpolation between two consecutive stages and the constraints of interest, including jerk and torque rate, are verified at selected check points along such profiles. This way, the search space does not need to be augmented and the complexity can be controlled without exiting the phase plane. Here, we essentially adopt the same solution, but the type of interpolation is left as a user choice as an additional mean to control the complexity. In both cases, when higher-order constraints are checked without augmenting the search space, the global optimality might be compromised [18].

Furthermore, with respect to pure redundancy resolution at kinematic level and pure time-optimal planning for non-redundant robots, the TOTP-R search space is of an increased dimension. Practically, this rules out the usage of an arbitrarily fine discretization. Therefore, our solutions might be, in some cases, far from the true global optimum, and we should rely on a more relaxed condition of *resolution-optimality*. A proof of convergence of approximate dynamic programming, for the more generic case of multi-objective optimization, is provided in [20].

IV. EXPERIMENTAL RESULTS

A. Experimental setup

The TOTP-R algorithm is validated on the Panda 7-DOF manipulator by Franka Emika¹, whose joint-space constraints

¹<https://www.franka.de/panda>

TABLE I

PANDA LIMITS FROM JOINT 1 (TOP) TO JOINT 7 (BOTTOM)

q_{min} [rad]	q_{max} [rad]	\dot{q}_{max} [rad/s]	\ddot{q}_{max} [rad/s ²]	\dddot{q}_{max} [rad/s ³]	τ_{max} [Nm]	$\dot{\tau}_{max}$ [Nm/s]
-2.8973	2.8973	2.1750	15	7500	87	1000
-1.7628	1.7628	2.1750	7.5	3750	87	1000
-2.8973	2.8973	2.1750	10	5000	87	1000
-3.0718	-0.0698	2.1750	12.5	6250	87	1000
-2.8973	2.8973	2.6100	15	7500	12	1000
-0.0175	3.7525	2.6100	20	10000	12	1000
-2.8973	2.8973	2.6100	20	10000	12	1000

are reported in Table I². We rely on the dynamic model identified in [23] and related libraries.

The redundancy parameter is selected as the joint position q_4 (middle of the chain), because it simplifies the analytical inverse kinematics in (7) [24]. As far as the discrete approximations for derivatives are concerned, in our experiments, that are based on a single-threaded implementation, we select a simple backward Euler approximation so as to speed up the computation and consume less memory. However, with a high-performance implementation, more complex discrete approximations could be used and more accurate results should be expected.

B. Planning

Two paths are designed in the workspace. One is a straight line path having $x = 0.5$ m, $z = 0.4$ m and y spanning for 0.5 m from $y_s = 0.25$ m to $y_e = -0.25$ m. The other is an ellipse-like line with $L = 1.45$. The end-effector orientation can be easily understood from the videos in [25]. Both tasks constrain six dimensions, leaving one degree of freedom for redundancy resolution. In addition, the robot has to track the path as fast as possible and is free to select the extended aspect (index g) that allows for the shortest tracking time: no extended aspect is excluded beforehand and the robot can possibly visit more than one of them. The parameters of the algorithm are selected as a result of a trade-off between computation time and accuracy.

The TOTP-R algorithm is executed on the straight line path and the results for different sets of parameters are reported in Table II. PV stands for *pseudo-velocity*, RP stands for *redundancy parameter*. Together with the cost, the trajectory percentage for which at least one actuator saturates is reported. Since a necessary condition for global optimality is that at least one actuator saturates for each waypoint, globally-optimal solutions should report a saturation of 100%. The first waypoint is excluded in the computation of the saturation percentage because it never saturates by construction, i.e. the manipulator always starts its motion with all quantities equal to zero.

The first aspect that we may notice, by looking at Table II, is that the optimal cost consistently is in a neighborhood of 0.6 s, with a variability of a few milliseconds. By increasing the number of waypoints only (see plans 4-6), the cost may increase or decrease. We should remark that more waypoints correspond to more constraints along the path and less freedom in deviating from the true straight line. On the other

TABLE II

RESULTS OF THE TOTP-R ALGORITHM ON THE STRAIGHT LINE PATH

Plan ID	Number of waypoints	PV limit	RP res. (deg)	PV res.	Cost (s)	Saturation (%)
1	10	1.4	0.500	0.02	0.655	100
2	10	1.4	0.250	0.02	0.594	89
3	10	1.4	0.250	0.01	0.592	89
4	10	1.4	0.125	0.02	0.574	89
5	15	1.4	0.125	0.02	0.645	100
6	20	1.4	0.125	0.02	0.602	95

hand, more waypoints allow to reduce the error related to the linear approximation that we make at each step by using a simple Euler integration scheme. As expected, with a fixed number of waypoints, the cost decreases for finer resolutions of the redundancy parameter and the pseudo-velocity (see plans 1-4), although the improvement due to the latter, in our experiments, is negligible (see plans 2 and 3).

The actuation limits of the Panda robot (see Table I), in our experiments, are always such that constraints in (16)-(17) activate before constraints in (18)-(20). This is also due to the fact that planning is performed by considering zero load at the end-effector, while jerk limits are very large. The resolution-optimal joint-space solution for plan 6 is reported in Fig. 1, its kinematic derivatives in Fig. 2, torques and their derivatives in Fig. 3. The computation time needed to find such a solution is 219 minutes on a 64-bit Ubuntu 18.04 LTS OS running on an Intel[®] Core[™] i7-2600 CPU @ 3.40GHz \times 8. This is the longer computation time among the plans in Table II. The TOTP-R algorithm in Fig. 1 has been implemented in C++ over ROS³ and MoveIt⁴. No multi-core execution model has been used in the experiments.

The reader may notice that, at first, joint 1's acceleration saturates to reach the maximum velocity, which persists for a large portion of the trajectory, between $t = 0.16$ s and $t = 0.37$ s. Here, there is a rather simultaneous saturation of joint 4's acceleration and joint 7's velocity, up until $t = 0.44$ s. In the last segment, joint 1's acceleration saturates again, followed by joint 2's acceleration to perform the final braking. For some segments of the trajectory, two constraints are active at the same time, which is expected for a redundant manipulator with $r = 1$, as argued in [7].

The phase plane trajectory, that in the case of TOTP-R is a *phase space trajectory (PST)*, is reported in Fig. 4. As noted above, for redundant manipulators, the PST is a function of two independent variables that are λ (the progress along the path) and \mathbf{v} , the redundancy parameter(s). The 3D view provides an indication of how the DP algorithm exploits the redundancy parameter to increase the pseudo-velocity and consequently compute a better solution with respect to a pre-assigned joint-space path.

The best parameters for the straight line path are directly re-used for the ellipse-like path, to assess their consistency across different paths. Since the path is longer ($L = 1.45$ m), a higher number of waypoints should be used to keep a similar spatial resolution. The parameters used for this use case are reported in Table III, together with the optimal cost

²<https://frankaemika.github.io/docs/>

³<https://www.ros.org/>

⁴<https://moveit.ros.org/>

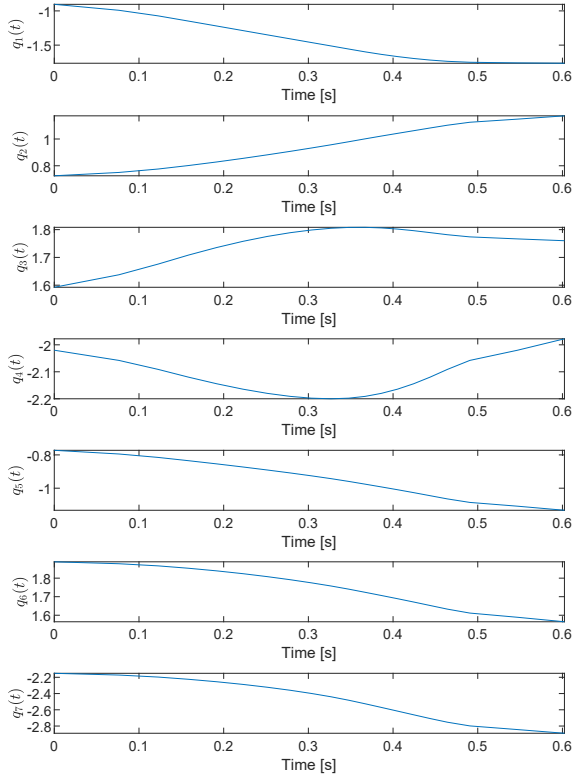


Fig. 1. Optimal joint positions for plan 6 of the straight line path.

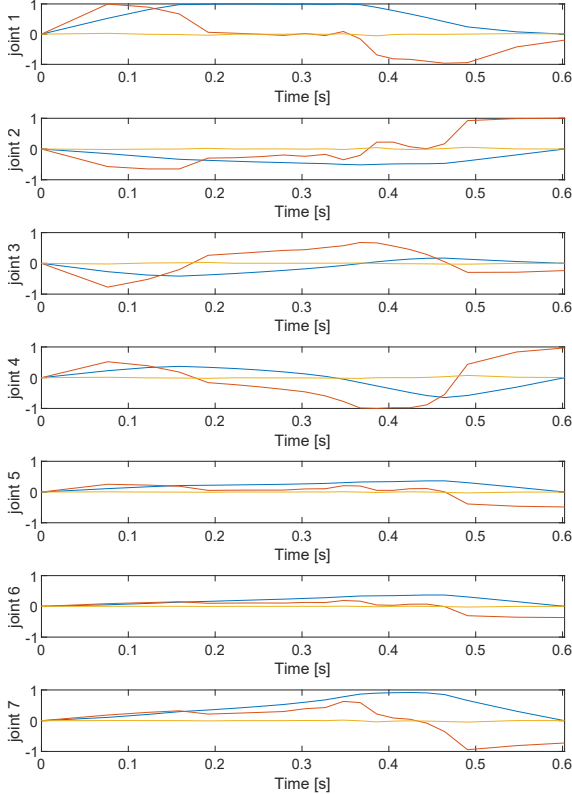


Fig. 2. Optimal joint velocities (blue), accelerations (red), and jerks (yellow) for plan 6 of the straight line path, normalized in $[-1, 1]$.

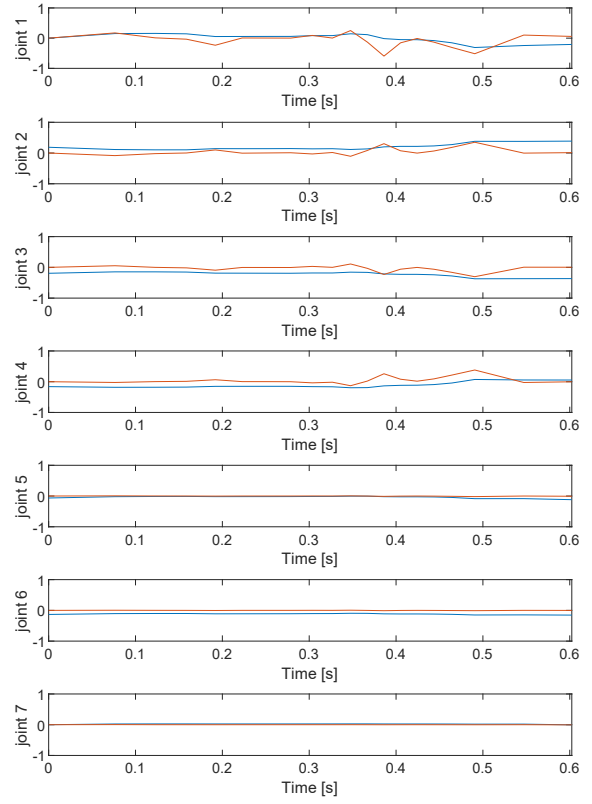


Fig. 3. Optimal joint torques (blue) and torque rates (red) for plan 6 of the straight line path, normalized in $[-1, 1]$.

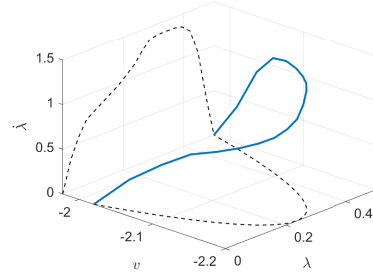


Fig. 4. Phase space trajectory (blue) with projections (black) on planes λ - λ and λ - v .

and percentage of saturation. Graphs are omitted for the sake of brevity, but similar results are obtained.

Since we do not have the true minimum time trajectory available, we compare our DP algorithm with a 2-stages approach from the literature, in order to assess the gain in performance given by the unified approach proposed in this paper. The same ellipse-like path is inverted and time-parametrized with the algorithm in [1]. Each workspace way-point is inverted through the local Jacobian-based iterative optimization scheme

$$\mathbf{q}_{k+1}(i) = \mathbf{q}_k(i) + \beta \mathbf{J}_k^\dagger \mathbf{e}_k - \alpha (\mathbf{I} - \mathbf{J}_k^\dagger \mathbf{J}_k) \nabla_{\mathbf{q}} c_k \quad (25)$$

where k is the iteration index, \mathbf{J}^\dagger is the $n \times m$ full-rank Moore-Penrose pseudo-inverse of the manipulator's geometric Jacobian, \mathbf{e}_k is the $m \times 1$ pseudo-twist Cartesian error vector, \mathbf{I} is the identity matrix of appropriate dimension,

TABLE III

RESULTS OF THE TOTP-R ALGORITHM ON THE ELLIPSE-LIKE PATH WITH SAME PARAMETERS AS PLAN 6 OF TABLE II.

Length (m)	Number of waypoints	PV limit	RP res. (deg)	PV res.	Cost (s)	Saturation (%)
1.45	60	1.4	0.125	0.02	1.856	90

$\nabla_{\mathbf{q}} c_k$ is the gradient of the cost function c selected for redundancy resolution, $\alpha = 10^{-4}$ and $\beta = 10^{-1}$ are gains on the null-space and Cartesian space correction terms, chosen after several trials. The cost is the projection of the dynamic manipulability ellipsoid onto the path's tangent \mathbf{t} , that is associated to the acceleration/deceleration capabilities of arm along the path [1]:

$$c(\mathbf{q}) = \mathbf{t}^T (\mathbf{H}\mathbf{J}^\dagger)^T \mathbf{H}\mathbf{J}^\dagger \mathbf{t}. \quad (26)$$

After the joint-space path has been obtained, it is time-parametrized with the algorithm from [16], by using the same pseudo-velocity limit and a pseudo-velocity resolution of 0.01. The trajectory tracking time is 2.557 s, about 38% higher than the unified approach.

C. Execution

Time-optimal methods are focused on planning, but, when time-optimal trajectories have to be fed to controllers, additional issues arise. In this section, it is our aim to demonstrate that, despite the approximations introduced by the discretization in the space and in the state domains, the trajectories generated with our DP algorithm can be executed on a real robot with satisfactory results.

The execution of the TOTP-R algorithm generates several control signals, as seen in Fig. 2 and Fig. 3. Before they can be used as commands for the Panda robot, it is necessary to interpolate them at the frequency of the controller, i.e. 1 kHz. Ideally, since the performed planning considers the manipulator's dynamic model, commands should be provided as open-loop torques. However, interpolating them in a post-processing stage will introduce errors that ultimately degrade performance in terms of tracking accuracy. Also, the Panda's torque controller interface requires net torques to be sent to the actuators, meaning that the efforts in Fig. 3 should be further post-processed to remove gravity and friction contributions.

Alternatively, the robot can be commanded with joint positions and control torques be generated with an internal controller. Position control has already been used in other works, e.g. [3], dealing as well with execution of time-optimal joint-space solutions, with satisfactory results. Furthermore, many robots do not allow for torque commands for safety reasons. Therefore, the analysis of the issues related to the usage of position commands is of utmost practical interest.

A high-level description of the control setup is shown in Fig. 5. As mentioned, the TOTP-R algorithm is deployed as a ROS/MoveIt! node. The controller manager of `ros_control`⁵ is configured to load a robot-agnostic joint trajectory controller (JTC), which performs quintic

⁵http://wiki.ros.org/ros_control

interpolation on the input signals to deliver smoother signals to the robot driver.

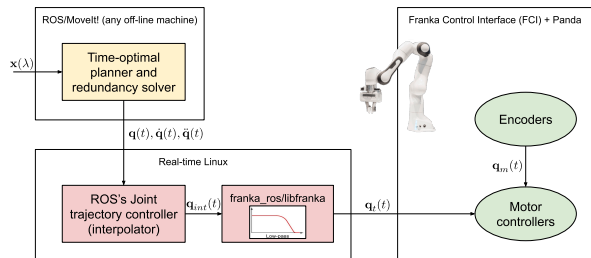


Fig. 5. Block diagram showing the control setup.

Notoriously, quintic interpolators might generate high-frequency oscillations. Since the JTC has no information about the specific robot, such oscillations are likely to violate kinematic and dynamic limits [18]. Several techniques exist to perform interpolation of control signals and still generate curves that are within bounds. In this case, we exploit some basic signal processing functions that are already provided by the manufacturer, i.e. a low-pass filter and a rate limiter. In particular, both of them are active to deliver less oscillating commands and ensure compliance to actuator limits. The employment of a filter to smooth out the trajectory is also beneficial to eliminate the high frequency content that excites the unmodeled joint elasticity that characterizes joints transmission in time-optimal control [26].

A comparison between planned joint positions and measured ones for the ellipse-like trajectory is reported in Fig. 6. The robot completes the motion in 1.859 s, 0.13% greater than planned with a maximum error in joint space of 0.8 deg. A video of the execution can be found in [25]. The tracking time of the same planned trajectory is scaled to be 10% shorter and the trajectory is executed again to estimate the performance. In this case, the motion is completed in 1.70 s, 0.67% greater than planned, with a maximum error of 1.86 deg, associated to joint 1 at $t = 0.11$ s. As expected, the robot cannot be controlled beyond its capacities and the actual motion results in a remarkable degradation of tracking performances.

V. CONCLUSIONS

In this paper, a DP framework has been presented for kineto-dynamic planning of redundant robots along prescribed paths. The framework unifies redundancy resolution and trajectory planning so as to solve them together to effectively utilize kinematic redundancy to optimize the objective function defined at trajectory planning level. The extreme flexibility of DP has been exploited to accommodate generic constraints that characterize real applications. DP ensures resolution-optimality, i.e. the asymptotic achievement of the globally-optimal solution as the discretization step tends to zero.

Although it is perfectly suited to solve one or the other problem separately, DP still requires hours to days to solve a medium-complexity planning problem for redundant robots and, most importantly, it is not scalable for systems characterized by a higher degree of redundancy, i.e. $r > 1$.

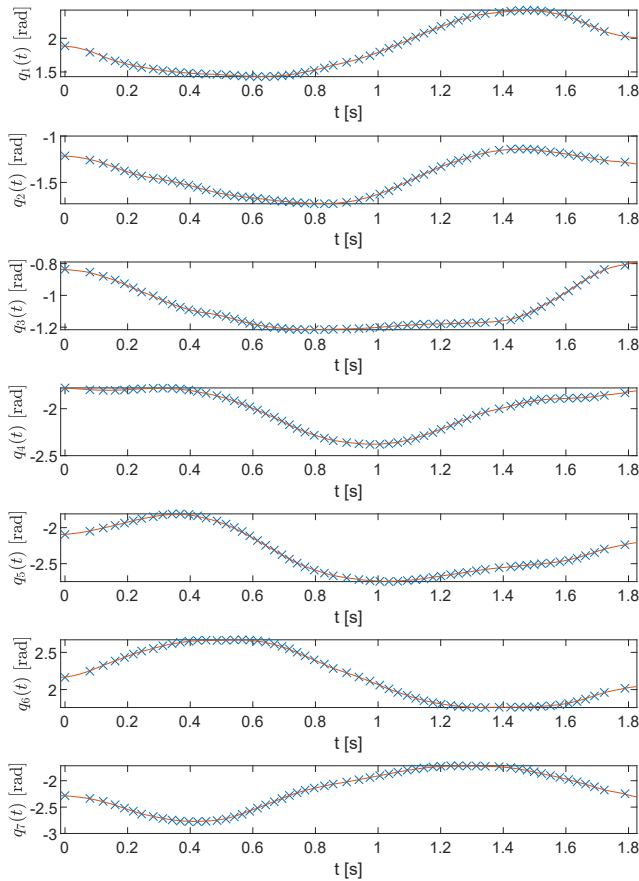


Fig. 6. Planned (blue crosses) vs measured (red line) joint positions for the ellipse-like trajectory.

Also, if one wanted to impose constraints on higher-order derivatives and, at the same time, preserve global-optimality, the phase space should be further augmented with additional dimensions. Again, DP is not scalable to this respect.

In light of these considerations, future developments might regard a deeper study into 2-stage techniques to understand whether some specific objective functions can be used for redundancy resolution (e.g., acceleration capability of the manipulator) that allow optimizing trajectory planning at a later stage. Also, it should be investigated whether global-optimality can be beneficial to this respect, in place of the local optimization methods discussed in [1], [2], [3].

ACKNOWLEDGMENT

The authors would like to thank Simon Lacroix for kindly supporting the setup of the experiments.

REFERENCES

- [1] P. Chiacchio, "Exploiting redundancy in minimum-time path following robot control," in *1990 American Control Conference*. IEEE, May 1990, pp. 2313–2318.
- [2] F. Basile and P. Chiacchio, "A contribution to minimum-time task-space path-following problem for redundant manipulators," *Robotica*, vol. 21, no. 2, pp. 137–142, February 2003.
- [3] K. Al Khudir and A. De Luca, "Faster motion on cartesian paths exploiting robot redundancy at the acceleration level," *IEEE Robotics and Automation Letters*, vol. 3, no. 4, pp. 3553–3560, October 2018.
- [4] J. E. Bobrow, S. Dubowsky, and J. S. Gibson, "Time-optimal control of robotic manipulators along specified paths," *The International Journal of Robotics Research*, vol. 4, no. 3, pp. 3–17, September 1985.

- [5] K. Shin and N. McKay, "Minimum-time control of robotic manipulators with geometric path constraints," *IEEE Transactions on Automatic Control*, vol. 30, no. 6, pp. 531–541, June 1985.
- [6] F. Pfeiffer and R. Johanni, "A concept for manipulator trajectory planning," *IEEE Journal on Robotics and Automation*, vol. 3, no. 2, pp. 115–123, April 1987.
- [7] M. Galicki and I. Pajak, "Optimal motions of redundant manipulators with state equality constraints," in *Proceedings - IEEE International Symposium on Assembly and Task Planning (ISATP'99)*. IEEE, July 1999, pp. 181–185.
- [8] M. Galicki, "Time-optimal controls of kinematically redundant manipulators with geometric constraints," *IEEE Transactions on Robotics and Automation*, vol. 16, no. 1, pp. 89–93, 2000.
- [9] S. Ma and M. Watanabe, "Time optimal path-tracking control of kinematically redundant manipulators," *JSME International Journal Series C*, vol. 47, no. 2, pp. 582–590, 2004.
- [10] A. Reiter, A. Müller, and H. Gattringer, "On higher order inverse kinematics methods in time-optimal trajectory planning for kinematically redundant manipulators," *IEEE Transactions on Industrial Informatics*, vol. 14, no. 4, pp. 1681–1690, April 2018.
- [11] A. P. Pashkevich, A. B. Dolgui, and O. A. Chumakov, "Multiobjective optimization of robot motion for laser cutting applications," *International Journal of Computer Integrated Manufacturing*, vol. 17, no. 2, pp. 171–183, March 2004.
- [12] A. Dolgui and A. Pashkevich, "Manipulator motion planning for high-speed robotic laser cutting," *International Journal of Production Research*, vol. 47, no. 20, pp. 5691–5715, July 2009.
- [13] A. Guigue, M. Ahmadi, R. Langlois, and M. J. D. Hayes, "Pareto optimality and multiobjective trajectory planning for a 7-dof redundant manipulator," *IEEE Transactions on Robotics*, vol. 26, no. 6, pp. 1094–1099, December 2010.
- [14] J. Gao, A. Pashkevich, and S. Caro, "Optimization of the robot and positioner motion in a redundant fiber placement workcell," *Mechanism and Machine Theory*, vol. 114, pp. 170–189, August 2017.
- [15] E. Ferrentino and P. Chiacchio, "On the optimal resolution of inverse kinematics for redundant manipulators using a topological analysis," *Journal of Mechanisms and Robotics*, vol. 12, no. 3, June 2020.
- [16] K. Shin and N. McKay, "A dynamic programming approach to trajectory planning of robotic manipulators," *IEEE Transactions on Automatic Control*, vol. 31, no. 6, pp. 491–500, June 1986.
- [17] S. Singh and M. C. Leu, "Optimal trajectory generation for robotic manipulators using dynamic programming," *Journal of Dynamic Systems, Measurement, and Control*, vol. 109, no. 2, pp. 88–96, 1987.
- [18] D. Kaserer, H. Gattringer, and A. Müller, "Nearly optimal path following with jerk and torque rate limits using dynamic programming," *IEEE Transactions on Robotics*, vol. 35, no. 2, pp. 521–528, April 2019.
- [19] —, "Time optimal motion planning and admittance control for cooperative grasping," *IEEE Robotics and Automation Letters*, vol. 5, no. 2, pp. 2216–2223, April 2020.
- [20] A. Guigue, M. Ahmadi, M. J. D. Hayes, and R. G. Langlois, "A discrete dynamic programming approximation to the multiobjective deterministic finite horizon optimal control problem," *SIAM Journal on Control and Optimization*, vol. 48, no. 4, pp. 2581–2599, January 2009.
- [21] A. Reiter, A. Müller, and H. Gattringer, "Inverse kinematics in minimum-time trajectory planning for kinematically redundant manipulators," in *IECON 2016 - 42nd Annual Conference of the IEEE Industrial Electronics Society*. IEEE, October 2016, pp. 6873–6878.
- [22] H. Pham and Q.-C. Pham, "On the structure of the time-optimal path parameterization problem with third-order constraints," in *2017 IEEE International Conference on Robotics and Automation (ICRA)*. IEEE, May 2017.
- [23] C. Gaz, M. Cognetti, A. Oliva, P. Robuffo Giordano, and A. De Luca, "Dynamic identification of the Franka Emika Panda robot with retrieval of feasible parameters using penalty-based optimization," *IEEE Robotics and Automation Letters*, vol. 4, no. 4, pp. 4147–4154, October 2019.
- [24] R. Diankov, "Automated construction of robotic manipulation programs," Ph.D. dissertation.
- [25] E. Ferrentino and H. Judiss Savino. (2020) Execution of time-optimal trajectories with Franka Emika's Panda robot. [Online]. Available: <https://www.youtube.com/watch?v=9xStJSPJ3bM>
- [26] J. Kim and E. A. Croft, "Online near time-optimal trajectory planning for industrial robots," *Robotics and Computer-Integrated Manufacturing*, vol. 58, pp. 158–171, August 2019.